Deep Learning for Path Loss Prediction in the 3.5 GHz CBRS Spectrum Band

Thao T. Nguyen, Raied Caromi, Kassem Kallas, and Michael R. Souryal‡
National Institute of Standards and Technology, Communications Technology Laboratory, USA
Email: {thao.t.nguyen, raied.caromi, kassem.kallas}@nist.gov

***Abstract*—In the 3.5 GHz Citizens Broadband Radio Service (CBRS) band, accurate path loss prediction is very important to protect the incumbent from harmful interference caused by the lower tier users. The current CBRS standards developed by the Wireless Innovation Forum use the irregular terrain model (ITM), also known as the Longley-Rice model, for path loss calculation. However, the model does not include clutter data, and thus, it underestimates the path loss. This paper utilizes a model-aided deep learning (DL) technique with satellite images to improve path loss prediction. Numerical study shows that the proposed approach can achieve a 4.23 dB root mean square error (RMSE) and outperform the Longley-Rice model and some tuned or fitted propagation models.**

I. Introduction

Accurate wireless propagation models are essential for wireless communication system planning and interference assessment, especially in frequency bands with spectrum sharing. Although numerous models have been developed for different environments and at different frequency bands (e.g., 900 MHz, 2.4 GHz, and 5.8 GHz) [1], [2], selecting an appropriate model to use is not always an easy task. The performance accuracy of each model often requires high computational complexity to achieve satisfactory results. The studies in [1], [2] found that typical best-case performance accuracy of the models is (12 to 15) dB root mean square error (RMSE). Models that are tuned or fitted with measurements can reduce the RMSE to (8 to 9) dB.

Citizens Broadband Radio Service (CBRS) in the 3.5 GHz band uses the common irregular terrain model (ITM)—also known as the Longley-Rice model—to compute the path loss for incumbent protection [3]. The Longley-Rice model takes into account the variations in terrain height between the transmitter and receiver, but it does not include clutter data in the path loss calculation. Thus, it is a conservative model, which may cause the spectrum to be underutilized by commercial operators.

Recent research on path loss prediction has focused on leveraging machine learning and deep learning (DL) to improve the performance accuracy with manageable computational complexity. An overview of machine learning techniques for propagation modeling is provided in [4]. In [5], [6], the authors use principal component analysis (PCA) and artificial neural networks (ANNs) to reduce the number of environment features and to learn the path loss, respectively. The authors in [7] utilize a DL encoder-decoder architecture to extract semantic information from satellite imagery to divide an area into urban, suburban, and rural environments, and then compute the path loss for each environment with the appropriate Okumura-Hata model. With a different approach, the authors in [8] use the DL VGG-16 architecture to predict path loss distribution of an area from satellite images. Although these techniques are interesting, we found the approach proposed by [9] compelling and closely related to our work. The proposed model in [9] is a hybrid model which combines both modeling-based and learning-based techniques for path loss prediction in the 2.6 GHz band. The modeling-based model, also called as a physics-based model, relies on a simple empirical path loss model to compute the received power estimate between the transmitter and the receiver. On the other hand, the learning-based model is a neural network (NN) that learns the surrounding environment's features from satellite images and geographical coordinates in order to provide a correction to the estimated received power. The sum of the received power estimate and the correction results in a prediction of received signal strength at the receiver.

In this paper, we aim to use a DL technique to predict the path loss for the 3.5 GHz CBRS band in the U.S. Our main contributions are summarized as follows:

- We modify the model-aided DL method in [9], especially the physics-based model, for path loss prediction in the 3.5 GHz CBRS band.
- We generate a large synthetic dataset representing San Diego, CA, to train the model. We apply transfer learning to fine-tune the pretrained model with a smaller real measurement dataset collected in the same area.
- We demonstrate that the proposed model outperforms the Longley-Rice model and tuned models.

The remainder of the paper is organized as follows. In Section II, we describe the NN approach for path loss prediction. Section III details how we generate datasets for training and testing the model. We present numerical results using both synthetic datasets and real measurements in Section IV. Finally, we summarize our results and provide conclusion remarks in Section V.

II. Neural Network Approach

In this section, we describe the DL model for path loss prediction in the 3.5 GHz band. We utilize and modify the

‡This paper is dedicated to the memory of Dr. Michael Souryal (1968–2020).

model-aided DL approach, which was developed in [9] for 2.6 GHz band, so that it can be suitable for the 3.5 GHz band. The proposed approach utilizes both modeling-based and DL techniques to predict the signal strength at each receiver location. The goal is to develop a regression model that can provide more accurate prediction results at unseen receiver locations than most traditional propagation models. In a simple scenario with one transmitter and one receiver, the received power can be computed as follows [10]

$$z = P_t + G_t + G_r - L \tag{1}$$

where z is the received power at the output of the receiver antenna (dBm) (dBm is expressed in decibels (dB) relative to one milliwatt (mW)), P_t is the transmit power at the transmitter (dBm), G_t and G_r are respectively the transmitting and receiving antenna gains (dBi), and L is the median path loss from the transmitter to the receiver (dB). Note that in this paper, we use the terms signal strength prediction and path loss prediction interchangeably since they can be derived from one another using Eq. (1).

We summarize the DL model below, but detailed information can be found in [9]. Fig. 1 shows an adapted version of the model-aided DL architecture. Inputs to the model include:

- d: distance between the transmitter and receiver,
- $x = [lat_{rx}, lon_{rx}, d, d_{lat}, d_{lon}, B_{tx}]$: engineered features, where lat_{rx} and lon_{rx} are the respective receiver coordinates in latitude and longitude, d_{lat} and d_{lon} are the respective distances in latitude and longitude between the transmitter and receiver, d is the distance, and B_{tx} indicates the transmitter of interest in a multi-transmitter scenario,
- A: satellite image, 256 pixel $\times$ 256 pixel ($\approx$ 185 m $\times$ 185 m), centered at the receiver location and rotated by an angle equal to the bearing between transmitter and receiver.

Given these inputs, the DL model learns the corrected received signal strength p at the receiver. The model architecture consists of two main components, i.e., a physics-based model and a correction NN. This hybrid approach combines expert knowledge from physics-based model and learning knowledge from the correction NN. Together, they improve the prediction performance.

A. Physics-based Model

The physics-based model is used to assist in the learning process. The model estimates the received power z from the distance d. It relies on the 3rd Generation Partnership Project (3GPP) empirical channel model in Urban Macro (UMa) scenario [11], which is identical to the International Telecommunication Union Radiocommunication Sector (ITU-R) M.2412 channel model in UMa_B scenario [12], to compute the median path loss L between the transmitter and receiver. Then, the physics-based model uses the link budget equation in Eq. (1) to estimate the received power z. Note that, besides the distance d, the channel model also uses other input parameters (i.e., frequency, transmitter and receiver heights,

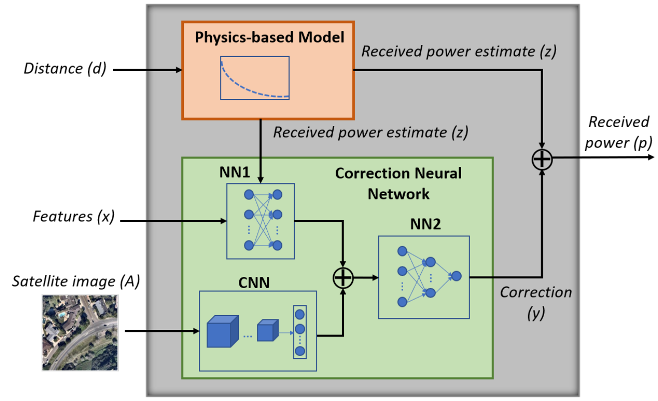

Fig. 1. A model-aided deep learning architecture, which consists of a physics-based model and a correction neural network, is used for predicting the received signal strength at the receiver.

and a calibration offset) to compute the path loss. However, these parameters are fixed values in this study; therefore, they are not shown as inputs in Fig. 1.

The received power estimate z will be concatenated with the engineered features x, and will be input to the correction NN to produce a correction factor y. In addition, the estimate z will be combined with the correction y to produce the final received power estimate $p = z + y$ as shown in Fig. 1.

B. Correction Neural Network

The correction NN consists of a convolutional neural network (CNN), and two fully connected neural networks NN1 and NN2. The CNN model is used to obtain features from the satellite image A. The NN1 model is used to manage the engineered features x and the received power estimate z. The outputs from the CNN and NN1 models will be added and input to the NN2 model. The last layer of NN2 is the output layer of the overall correction NN model, which learns the correction y. The Rectified Linear Unit (ReLU) and linear activation functions are used in the sub-models.

The model parameters are learned iteratively through the backpropagation algorithm with the mean square error (MSE) loss function criterion. We used the well-known Adam optimizer as well as mini-batch to speed up the training process. To avoid overfitting, we employed regularization techniques such as batch normalization, dropout, and weight decays. Moreover, we used image augmentation with a random rotation of the original image for improving generalization in this study, but other data augmentation techniques can be used as well. Generally, the search for hyper-parameters for a NN is computationally expensive and time consuming. Therefore, we reuse most of the tuned hyper-parameters in [9] and only adjust some parameters to suit our system's capability.

Table I shows the architectures and layer sizes of the CNN, NN1, and NN2 sub-models of the correction NN. It also lists the hyper-parameters used in this study.

TABLE I
CORRECTION NEURAL NETWORK MODEL PARAMETERS AND HYPERPARAMETERS USED FOR TRAINING THE MODEL.

	Parameter	Value
CNN	Input channel	1
	Number of convolutions	[200, 100, 50, 25, 12, 1]
	Activation	ReLU, Linear
	Kernel size	[(5,5), (3,3), (3,3), (3,3), (2,2), (2,2)]
	Max pooling	2
	Padding	2
	Stride	1
NN1	Layer size	[200, 200]
	Activation	ReLU, Linear
NN2	Layer size	[200, 16, 1]
	Activation	ReLU, Linear
Hyperparameter	Batch size	8
	Loss function	MSE
	Optimizer	Adam
	Weight decay	2.8e-3
	Learning rate	1e-3
	Image augmentation angle (max angle)	20

III. DATASET GENERATION

Besides the selection of learning algorithms, a large amount of curated and representative datasets is essential for the development of DL models. In this section, we describe our approach for generating training, evaluation, and test datasets for the proposed model-aided DL network. In particular, we discuss the real measurements, the simulated data, and our workflow.

A. Real Propagation Measurements

Real measurements are valuable in production of practical and functional models, but they are usually expensive and time-consuming to obtain. In this study, we utilize the real propagation measurements collected by the Institute for Telecommunication Sciences (ITS) [13]. Although the measurement campaigns were at different locations in the U.S. and at different frequency bands, in this analysis we focus on the 3505 MHz data collected in San Diego, CA. The transmitter was located near a parking lot on the Navy Point Loma submarine base. The transmitting power was approximately 40 dBm with an antenna height of approximately 10 m above ground level (AGL). The equipment used to collect the receiving signals was placed in a van and the receiver antenna height was approximately 3 m AGL. Transmitting and receiving antenna gains and cable losses contributed about 3 dB to the link budget calculation. Fig. 2 depicts the drive route near the neighborhood of Point Loma in San Diego. The van started at a location about 8 km away from the transmitter and then drove closer to it. The different colors along the route represent the received signal strengths received at receiver locations. The original dataset collected by ITS has 1200 data samples. After examining the measurements, we kept 994 samples (as shown in Fig. 2) and discarded the remaining receiver noise samples.

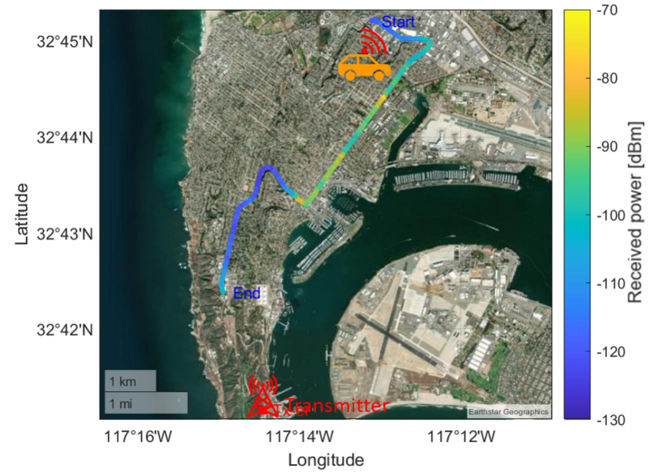

Fig. 2. Measurements drive route at 3505 MHz in San Diego, CA.

B. Synthetic Dataset

Given the insufficient quantity of real measurements for training the model, we need to generate a larger dataset that is representative and contains the same types of relevant features as the real measurements. We used the Mentum Planet tool[1] and replicated the San Diego measurement campaign. We used two propagation models, i.e., Longley-Rice and Universal models, to compute the path loss at all the grids within 50 km centered at the transmitter. Since the Longley-Rice model does not use clutter data in its calculation, we also consider the Universal model, which is an advanced propagation model developed in the Mentum Planet tool, for comparison purposes. Fig. 3 shows the path loss prediction of the Universal model (the left subplot) and the Longley-Rice model (the right subplot). In most cases, the Universal model predicts higher path losses than the Longley-Rice model. However, opposite prediction results are observed at locations in the sea area or locations more than 10 km from away from the transmitter.

After computing the path loss for the entire area, we extracted the values along the drive route shown in Fig. 2. We then computed the associated received signal strengths at these receiver locations. Fig. 4 shows the received power vs. distance of the real measurements (in orange), prediction by the Universal model (in red), and prediction by the Longley-Rice model (in purple). Utilizing both terrain and clutter data, the Universal model is capable of providing better prediction results with 7.16 dB RMSE than the Longley-Rice model with 14.42 dB RMSE. As a result, we used the path loss prediction by the Universal model for generating a large synthetic dataset.

To get more receiver locations in the San Diego area, we drew random routes using the Google Maps tool. Fig. 5 shows the blue routes to be used for training and the orange routes to

[1]Certain commercial equipment, instruments, or materials are identified in this paper to foster understanding. Such identification does not imply recommendation or endorsement by the National Institute of Standards and Technology, nor does it imply that the materials or equipment identified are necessarily the best available for the purpose.

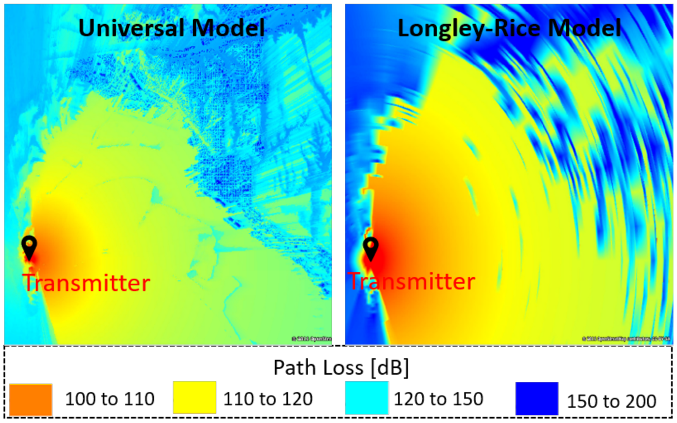

Fig. 3. Path loss generated by the Universal and Longley-Rice models.

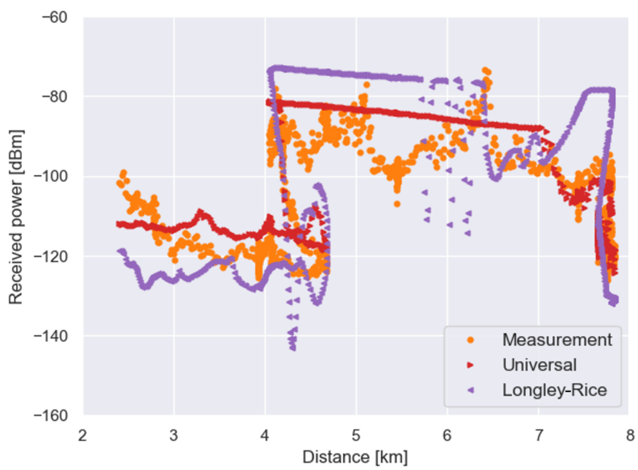

Fig. 4. Received signal power vs. distance of real measurements as well as predictions by the Universal and Longley-Rice models.

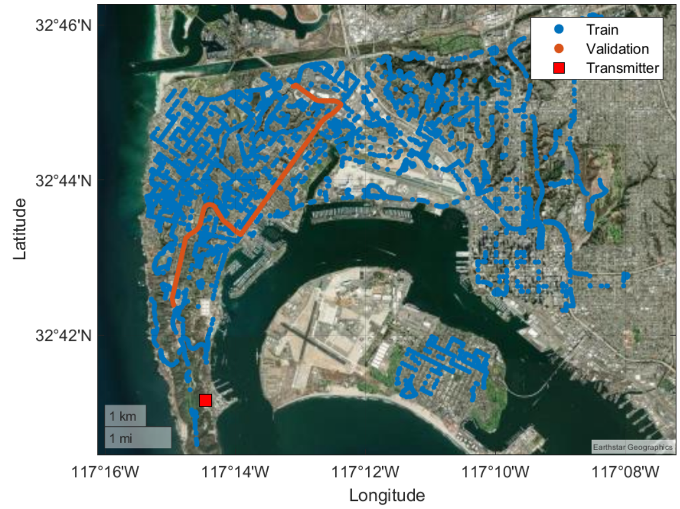

Fig. 5. Train and test routes used for generating synthetic datasets.

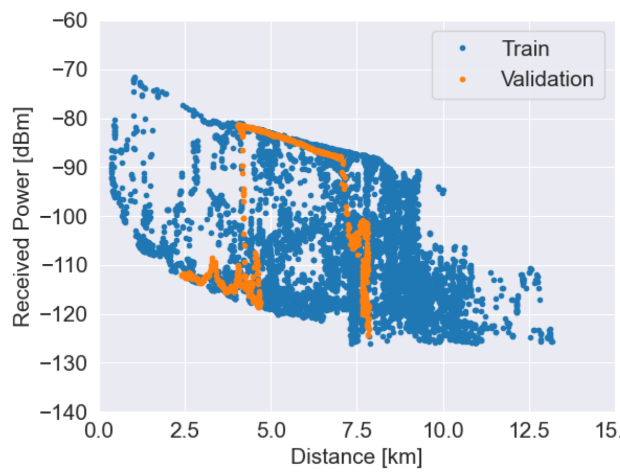

Fig. 6. Synthetic datasets for training the model-aided neural network.

be used for validating the model. There are 11 241 samples in total; 9982 samples and 1259 samples to be used for training and validation, respectively. Given these receiver locations, the Universal path losses and received signal strengths were computed in similar fashion to the results in Fig. 4 and we plot them in Fig. 6.

C. *Workflow*

Fig. 7 summarizes our workflow for this study. There are three main tasks including i) data generation, ii) data processing, and iii) model training, testing and performance evaluation. In the data generation task, we used the Universal model to generate path loss, Google Maps to generate test routes, the Mapbox tool to extract satellite images, and the real measurements to fine-tune and test the model. For the data processing task, we used MATLAB and Python to generate features and targets data and save them in .csv files, and to get satellite images at the receiver locations. The files constitute the synthetic dataset and the real measurement dataset. The synthetic dataset is for training and validation of the model. Once the model is trained, we fine-tune the pretrained model and test it with the real measurement dataset. The model training, testing, and performance evaluation task is performed in PyTorch.

IV. Results

In this section, we present results of the model-aided DL technique for path loss prediction in the 3.5 GHz band. We first show the pretrained model performance with synthetic dataset and then the fine-tuned model performance with real measurements.

A. *Training and Validation with Synthetic Datasets*

We trained and validated the DL model described in Section II with 50 epochs but the process stopped earlier at 43 epochs due to low learning rate. Fig. 8 shows the normalized mean squared error (MSE) at each epoch during the training and validation. As the number of epochs increases,

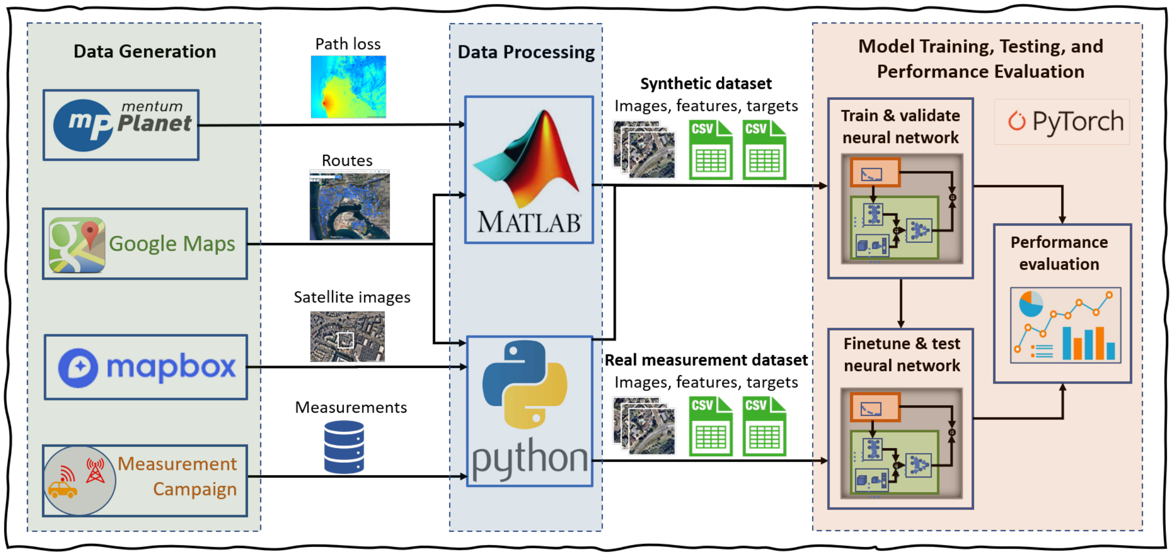

Fig. 7. A workflow shows the process used in this study including data generation, data processing, and model training, testing and performance evaluation.

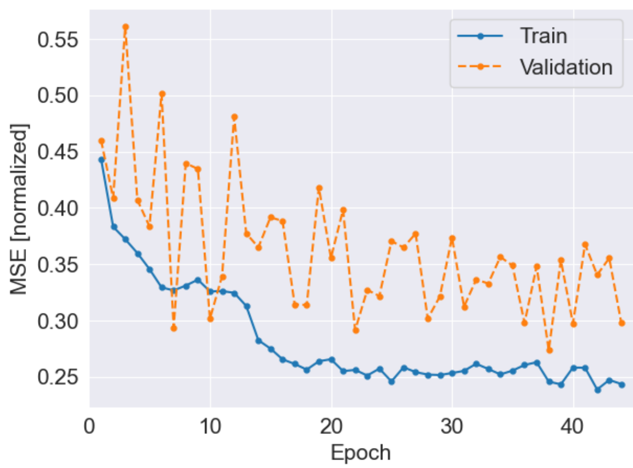

Fig. 8. Normalized mean square error (MSE) during training and testing of the deep learning model with synthetic datasets.

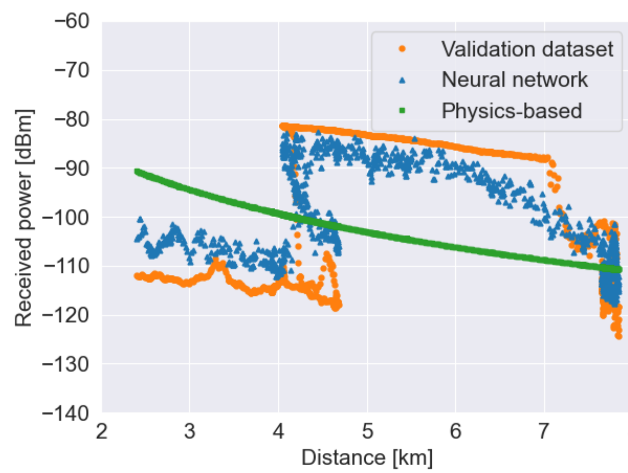

Fig. 9. Prediction results on the synthetic test dataset of the neural network and physics-based models.

the normalized MSE for training gradually decreases while the validation curve oscillates and decreases as well. Also, as mentioned in [9], using data augmentation and tuned regularization parameters reduces severe overfitting during training.

Fig. 9 shows the prediction results of the proposed NN (in blue) as well as the physics-based model alone (in green) against the target or validation data (in orange). While the physics-based model provides predictions in the middle between the two clusters of received power values in the target dataset, the NN situates predictions closer to the targets. To compare the predictive performances of the NN and the physics-based models, we computed the errors in terms of RMSE. The smaller the RMSE value is, the closer the prediction is to the target. The NN provides a very good RMSE of 7.08 dB, which is smaller than the (8 to 9) dB range provided by tuned or fitted models described in [1], [2]. As expected, the physics-based model gives a larger RMSE of 15.45 dB, which is near the upper bound of the (12 to 15) dB range of the typical best-case performance models shown in [1], [2]. Leveraging the learned correction using engineered features and satellite images, the model-aided NN is able to predict the target more accurately than the physics-based model alone.

B. Transfer Learning with Real Measurements

With the NN model pretrained on a large synthetic dataset, we applied transfer learning to fine-tune the model using 994 real measurement samples described in Section III-A. We reused all the pretrained layers and then fine-tuned them using 100 random samples from the real measurement dataset. We

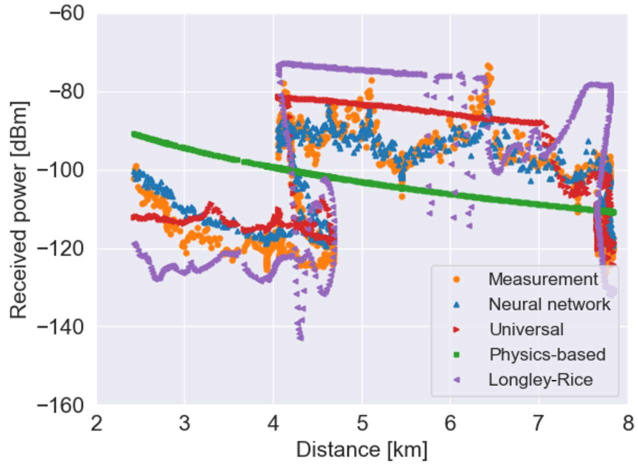

Fig. 10. Prediction results on real measurements for the neural network, Universal, physics-based, and Longley-Rice models.

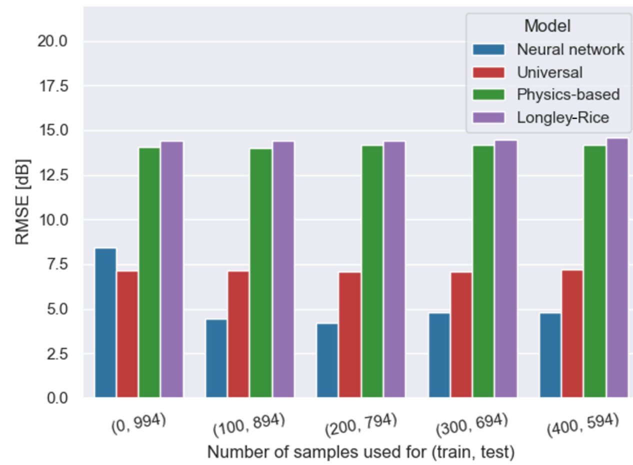

Fig. 11. RMSE prediction results with different sets of (train, test) for all models.

used the remaining 894 samples from the real measurement dataset to test the prediction performance of the model.

We compare the prediction performance of the NN with the other non-learning models used in this study. Fig. 10 shows the received power level vs. distance of the target test set (in orange), and predictions by the NN (in blue), the Universal model (in red), the physics-based model (in green), and the Longley-Rice model (in purple). The NN outperforms other models with RMSE of 4.46 dB; whereas the Universal, physics-based, and Longley-Rice achieve 7.16 dB, 13.98 dB, and 14.43 dB RMSE, respectively. Interestingly, the performance of the proposed NN for the 3.5 GHz band in this study is similar to the performance of the same model for the 2.6 GHz band in [9].

We varied the number of samples used for retraining and testing the NN and observed the predictive performance. Fig. 11 shows the RMSE at different sets of (train, test) for all models. Without fine-tuning, i.e., (train, test) = $(0, 994)$, the NN achieves a 8.42 dB RMSE, which is worse than the Universal model but still smaller than the physics-based and Longley-Rice models. As the number of training samples increases up to 300, the RMSE of the NN lowers to 4.23 dB, but no gain is observed after 300 training samples. Unlike the NN, which can be re-trained on new information, in this study, the Universal, the physics-based, and the Longley-Rice models predict the path loss only once. Therefore, the RMSE values provided by these traditional models do not vary much, i.e., (7.10 to 7.21) dB for the Universal model, (13.98 to 14.19) dB for the physics-based model, and (14.39 to 14.57) dB for the Longley-Rice model.

V. Conclusion

In this paper, we presented a model-aided DL technique, which combines both physics-based and learning-based techniques, to predict path loss in the 3.5 GHz band more accurately than traditional models. Using transfer learning, we achieved good prediction performance of 4.23 dB RMSE even with a limited dataset. For future work, we will incorporate 3D features such as building and vegetation heights into the model, and also extend it to predict path loss in the 6 GHz band.

References

[1] C. Phillips, D. Sicker, and D. Grunwald, "A survey of wireless path loss prediction and coverage mapping methods," *IEEE Communications Surveys and Tutorials*, vol. 15, no. 1, pp. 255–270, 2013.

[2] ——, "Bounding the error of path loss models," *IEEE International Symposium on Dynamic Spectrum Access Networks (DySPAN)*, pp. 71–82, 2011.

[3] "Requirements for commercial operation in the U.S. 3550–3700 MHz Citizens Broadband Radio Service band," Wireless Innovation Forum Document WINNF-TS-0112, Version 1.9.1, Mar. 2020. [Online]. Available: https://cbrs.wirelessinnovation.org/release-1-standards-specifications

[4] A. Seretis and C. D. Sarris, "An overview of machine learning techniques for radiowave propagation modeling," 2021. [Online]. Available: https://arxiv.org/pdf/2101.11760.pdf

[5] L. Wu, D. He, B. Ai, J. Wang, H. Qi, K. Guan, and Z. Zhong, "Artificial neural network based path loss prediction for wireless communication network," *IEEE Access*, 2020.

[6] H.-S. Jo, C. Park, E. Lee, H. K. Choi, and J. Park, "Path loss prediction based on machine learning techniques: Principal component analysis, artificial neural network and Gaussian process," *Sensors (Basel)*, 2020.

[7] M. E. Morocho-Cayamcela, M. Maier, and W. Lim, "Breaking wireless propagation environmental uncertainty with deep learning," *IEEE Transactions on Wireless Communications*, vol. 19, no. 8, 2020.

[8] O. Ahmadien, H. F. Ates, T. Baykas, and B. K. Gunturk, "Predicting path loss distribution of an area from satellite images using deep learning," *IEEE Access*, vol. 8, pp. 64 982–64 991, 2020.

[9] J. Thrane, D. Zibar, and H. L. Christiansen, "Model-aided deep learning method for path loss prediction in mobile communication systems at 2.6 GHz," *IEEE Access*, vol. 8, pp. 7925–7936, 2020.

[10] G. L. Stuber, *Principles of Mobile Communication (2nd edition)*. Kluwer Academic Publishers, 2001.

[11] "5G; Study on channel model for frequencies from 0.5 to 100 GHz," 3GPP TR 38.901, Version 14.0.0, Release 14, 2017.

[12] "Guidelines for evaluation of radio interface technologies for IMT-2020," Report ITU-R M.2412-0, 2017.

[13] C. Hammerschmidt and R. Johnk, "Extracting clutter metrics from mobile propagation measurements in the 1755-1780 MHz band," *MILCOM 2016 - 2016 IEEE Military Communications Conference*, 2016.